ISSN Print: 2394-7500
ISSN Online: 2394-5869
Impact Factor (RJIF): 8.69
IJAR 2025; 11(10): 314-317
www.allresearchjournal.com
Received: 19-08-2025
Accepted: 21-09-2025

Yong-Chol Choe
Mirae Institute of Industrial Technology, Kim Chaek University of Technology, Pyongyang, Democratic People's Republic of Korea

Myong-Gil Yun
Mirae Institute of Industrial Technology, Kim Chaek University of Technology, Pyongyang, Democratic People's Republic of Korea

Chun-Hyok Jong
Mirae Institute of Industrial Technology, Kim Chaek University of Technology, Pyongyang, Democratic People's Republic of Korea

Sung-Hyon Kim
Faculty of Nuclear Science and Technology, Kim Chaek University of Technology, Pyongyang, Democratic People's Republic of Korea

Choljin Jang
Mirae Institute of Industrial Technology, Kim Chaek University of Technology, Pyongyang, Democratic People's Republic of Korea

Corresponding Author:
Choljin Jang
Mirae Institute of Industrial Technology, Kim Chaek University of Technology, Pyongyang, Democratic People's Republic of Korea

Study on the high-performance transient electromagnetic system for tunnel detection

Yong-Chol Choe, Myong-Gil Yun, Chun-Hyok Jong, Sung-Hyon Kim and Choljin Jang

DOI: https://doi.org/10.22271/allresearch.2025.v11.i10d.12956

Abstract
Tunnel-detection TEM is an effective tool for exploration of anthracite coal and detection of flood accident in pit. The paper presents solutions for efficient use of limited power supply (batteries) while improving exploration accuracy in TEM system used for tunnel detection. They include the circuit for fast turn-off of transmitter current, the shielded receiver loop, and the selection method of optimal stacking-times. The experimental results show that these solutions are valuable in preventing unnecessary power increase, whole-space effect, and excessive stacking.

Keywords: Transient electromagnetic, fast turn-off, stacking-times, shield design, tunnel detection

Introduction
The TEM system used for tunnel detection generally has to meet the requirements of low-depth, high-resolution. It is a portable low-power apparatus, and uses batteries as power supply. Hence, it is important to improve exploration accuracy and power utilization efficiency in tunnel detection TEM system [1, 2].
Generally, to increase the S/N ratio, the transmitter current intensity increases, which leads to an increase in power consumption. For the same transmitter current, a shorter current turn-off time can result in a stronger response and thus improve the S/N ratio [3]. The transmitter circuit of literature [4] is an excellent solution based on constant voltage clamp technique, but the circuit configuration is complex and unsuitable for low power TEM systems.
Synchronous detection is a commonly used measurement scheme for suppression of DC offset noise and power-line noise in TEM system. However, if the stacking-times are taken too large, it will result in power dissipation due to unnecessary repeated measurements. Conversely, too small stacking-times results in insufficient noise suppression. Therefore, an optimal choice of the stacking-times is necessary to suppress the noise sufficiently and prevent power dissipation [5].
On the other hand, in tunnel detection TEM, because of the narrow opening space, a small loop is used, and the exploration accuracy is poor due to the whole space effect [6]. In particular, suppressing the backward interference from the opposite side of the aimed direction is important for accuracy improvement. In literature [7], a special receiver antenna with shield was used to prevent backward interference, but no detailed shielding structure was mentioned.
Hence, the paper proposes some solutions to effectively utilize limited power supply while improving exploration accuracy in tunnel detection TEM systems. They include a circuit scheme for fast linear turn-off of the transmitter current, a reasonable shielding structure of the receiver loop, and an optimal selection of the stacking-times.

Technical Solutions for tunnel-detection TEM
Fast turn-off of transmitter current
Figure 1 shows a simple and practical circuit scheme for fast linear turn-off of current in low power TEM transmitter. It is based on constant voltage clamping technique and loop splitting.

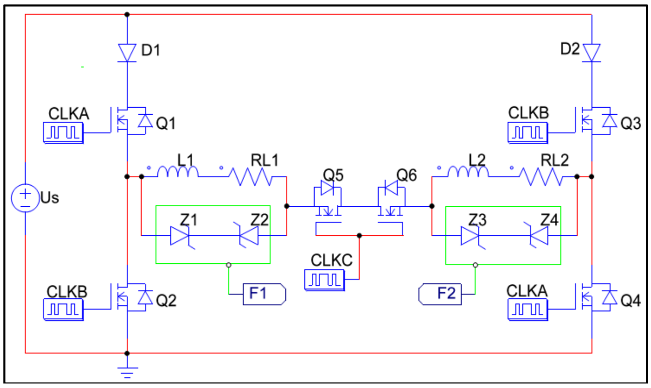

Fig 1: Fast turn-off circuit scheme for low power TEM transmitter.

In Figure 1, Z1~Z4 are transient voltage suppressors (TVS), which constitute passive constant voltage clamp circuits F1 and F2. The transmitter loop is divided into two equal parts at the moment of current off, where the inductance and the internal resistance are denoted as L1, RL1, L2, and RL2, respectively. Diodes D1 and D2 block the channel between the transmitter loop and the power supply Us when the current is turned off, so that the induced energy accumulated in the loop does not affect the power supply (battery).
The transmitter current rises exponentially due to the inductive load, which is expressed by

$$i_o(t) = I_0\left(1 - e^{-\frac{R_L}{L}(t-t_0)}\right) \qquad t_0 \le t < t_1 \quad , \quad (1)$$

Where t0 and t1 denote the switch-on and switch-off times of the transmitter current, respectively. In addition, L and RL are the total inductance and internal resistance of the integrated transmitter loop, and Io represents the load current value at steady state.
Then, at time t=t1, when all switches (Q1 to Q6) are turned off, the transmitter loop is divided into two equal parts. As the load energy is rapidly dissipated through the TVSs, the transmitter current io(t) drops rapidly and linearly. The load current during pulse dropping is expressed as

$$i_o(t) = -\frac{U_C}{R_L} + \left(I_0 + \frac{U_C}{R_L}\right)e^{-\frac{R_L}{L}(t-t_1)} \qquad t_1 \le t \le t_2. \quad (2)$$

Where, t2 is the time when io(t2)=0A, i.e. the time when the current is completely turned off.
From Eq. (2), the descent time td of the transmitter current pulse is

$$t_d = t_2 - t_1 = -\frac{L}{R_L}\ln\frac{U_C}{U_C + I_0 R_L}. \quad (3)$$

In general, the loop resistance RL is very small. From Eq. (3), it can be seen that if the clamp voltage UC is very large compared to I0RL, the drop time is greatly shortened.
Also, from Eq. (2), the slope of the pulse falling edge can be obtained:

$$\frac{di_o(t)}{dt} = -\frac{U_C + I_0 R_L}{L}e^{-\frac{R_L}{L}(t-t_1)} \qquad t_1 \le t \le t_2. \quad (4)$$

In Eq. (4), if the effect of the loop resistance RL is neglected, $di_o(t)/dt = -U_C/L$, i.e. the slope becomes constant, which means that the current pulse is linearly falling.
On the other hand, the inductance of loop can be calculated using the following formula [6]:

$$L = \mu_0/(4\pi)n^2 d\Phi \;, \quad (5)$$

where n is the turns of loop, d(m) is the diameter of loop, Φ is the intermediate variable, and μ0 is the permeability of the vacuum. When the transmitter loop is divided into two parts during the current pulse drop, the following relationship holds:

$$L_1 \approx L/4, \qquad L_2 \approx L/4 \;, \quad (6)$$

$$R_{L1} = R_{L2} = R_L/2. \quad (7)$$

Now, substituting Eqs. (6) and (7) into Eqs. (3) and (4), it can be seen that the descent time and the linearity are further improved by the loop splitting.

Shielded receiver loop

In tunnel detection TEM, the secondary field from the opposite side of the aimed direction also acts on the receiver loop, greatly reducing the sounding accuracy. We propose a shielded receiver loop as a way to suppress this backward interference.
In order to choose a suitable shielding structure, simulations were carried out using ANSYS Maxwell. Two shielding structures were considered in the simulation: one is to place a 0.5 mm thick Mn-Zn ferrite sheet on the outer surface of the receiver loop, and the other is to install a 0.1 mm aluminum foil with a 0.5 mm ferrite sheet. The simulation results show that the shielding effect of the second case is better.
Theoretical considerations of the simulation results are presented. Figure 2 shows the shielding mechanism of the two shielding structures mentioned above. In the first case, as shown in Figure 2a, most of the magnetic field incident perpendicular to the loop is concentrated in the ferrite sheet and propagates transversely, resulting in a weakening of the magnetic field behind the ferrite sheet. However, as part of the field penetrates the ferrite sheet, there is still a residual force. On the other hand, if an aluminum foil is added to the outside of the ferrite sheet, this residual field force induces a damped eddy current in the aluminum foil (Figure 2b). The inhibiting magnetic field produced by the eddy current has little effect on the loop because it propagates along the ferrite sheet. Thus, passing the ferrite sheet and the aluminum foil will greatly reduce the magnetic field strength and increase the shielding effect.

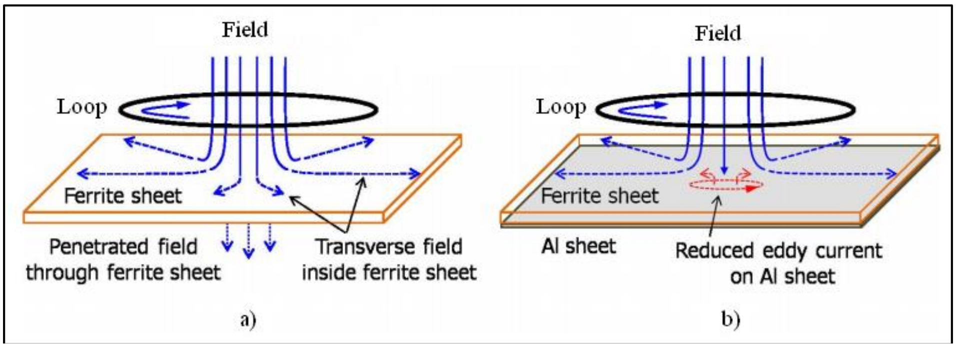

Fig 2: Shielding mechanism of different shielding structures.

Based on the simulation results, we selected the optimal shielding structure of the receiver loop as a three-layer structure of ferrite-aluminum-ferrite. If such a three-layer shield is mounted on the rear side of the receiver loop (the aimed direction is called the front), the backward interference can be greatly suppressed without compromising the receiving signal.

Optimal choice of stacking-times

In conventional TEM systems, including Geonics's PROTEM, the stacking-times is set subjectively by the user. However, excessive stacking-times result in unnecessary measurement time consumption and power dissipation. We used an optimal stacking-times determination algorithm [5] with power-line noise estimates and noise tolerance as input data.

In the scheme, when the base frequency fB of the TEM system is equal to Eq. (8), the stacking-times is equal to Eq. (9):

$$f_B = \frac{2p\text{-}1}{2q} \cdot f_P, \quad (8)$$

$$m_{stk} = (2p-1) \cdot l. \quad (9)$$

Where, fP is the power-line frequency, and p, q, and l are all natural numbers. For convenience, (2p-1) and 2q are considered to be mutually exclusive. The optimal stacking-times determination algorithm is based on Eq. (10):

$$\max_i(|E_i|) = \frac{1}{2(2p-1)l} \sum_k A_k \left| \frac{\sin\left(2\pi kql \cdot \Delta f_P / \hat{f}_P\right)}{\cos\left(\pi kq/(2p-1)\left(1+\Delta f_P / \hat{f}_P\right)\right)} \right|, \quad (10)$$

where Ak is the amplitude of the k-th harmonic of the power-line noise and k = 1, 3, 5, ~. In addition, $\hat{f}_P$ is the estimate of the power-line frequency, and Δf_P is the deviation between the actual value of the power-line frequency and the estimate. Also i is the sample number.

Eq. (10) actually represents the maximum amplitude of the residual power-line noise in the i-th sample after the mstk synchronous stacking process. When the noise tolerance is set to δ, it can be guaranteed that the power-line noise is sufficiently suppressed if the condition $\max_i(|E_i|) \le \delta$ is satisfied for any i. As known in Eq. (10), the function $\max_i(|E_i|)$ with respect to l is obviously damped as l increases. Thus, by determining the minimum value (lmin, a natural number) of l satisfying $\max_i(|E_i|) \le \delta$, we can determine the optimal stacking-times from Eq. (9).

Experimental Results and Discussion

To evaluate the performance of the proposed fast turn-off circuit, simulations were conducted by PSIM v9.0 software. The transmitter loop is a 32-turn square coil made by winding 1.5 mm^2 copper wire. A side length of it is 2 m long. The base frequency is f_B = 12.5 Hz and the supply voltage is U_S = 25.2 V. The clamping voltage is U_C = 548 V. Figure 3 shows the simulation results. In Figure 3 (a), (b), and (c), the current turn-off times are 810.3 us, 55.8 us, and 14.5 us, respectively. Finally, it can be seen that the proposed circuit scheme is the best. Meanwhile, the transmitter prototype was tested on the same loop as in the simulation. The actual turn-off time of the transmitter current is 14.7 us, which is almost the same as the simulation results.

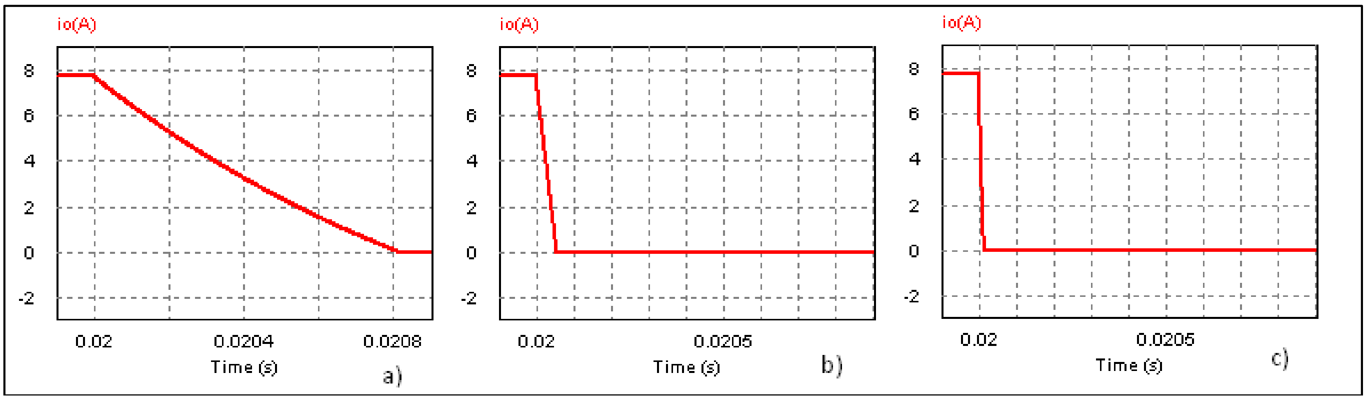

Fig 3: Comparison of the current falling edge for different transmitter circuits. (a) Traditional full-bridge inverter circuits. (b) Using only clamp circuit. (c) Proposed circuit.

The simulation results by ANSYS Maxwell show that the shield efficiency of the proposed scheme is about 120 dB, which can adequately suppress the backward interference in the tunnel.

On the other hand, when the power-line noise estimates is $\hat{A}_1 = 12.576\,m\text{V}$, $\hat{A}_3 = 5.274\,m\text{V}$, $\hat{A}_5 = 1.217\,m\text{V}$, $\hat{A}_7 = 0.159\,m\text{V}$, $\hat{A}_9 = 0.043\,m\text{V}$, $\hat{f}_P = 50.76\,Hz$ ($\Delta\bar{f}_P = 0.01\,Hz$), and the noise tolerance δ=2 uV, the selected optimal stacking-times is m_{stk} = 4,818. The experimental results show that after 4,818 stacking, the residual noise amplitude is 1.89 *uV*, which is below the acceptable limit.

The proposed circuit can only be applied to low power TEM due to the limitation of TVS. For the shielded receiver loop, the thicknesses of the ferrite and aluminum sheets (0.5 mm, 0.1 mm) are not the optimal value. The optimal stacking-times selection method can ensure its reliability when there is no change of power-line frequency or when the change is relatively slow.

Conclusion

We have proposed some technical solutions for tunnel detection TEM. First, we designed a fast turn-off transmitter circuit based on constant voltage clamping technique and loop splitting. Next, a receiver-loop shielding structure with three-layer sheets of ferrite-aluminum-ferrite is proposed for suppressing the backward interference. Also, the optimal stacking-times is chosen to suppress unstable power-line noise while preventing power dissipation due to excessive stacking. These solutions can be applied not only to tunnel detection but also to shallow-layer exploration on the ground. Future work will be directed to further improve the limitations of the proposed schemes.

Acknowledgments

The authors thank the editor and anonymous reviewers for valuable comment and advice.

References

1. Li H, Xue JJ, Fan KR, Li WH, Li X. Development of tunnel detection technology using the transient electromagnetic method in China. J Appl Geophys. 2025;105623.
2. Tang HZ, Yang HY, Lu GY, Chen SN, Yue JH, Zhu ZQ. Small multi-turn coils based on transient electromagnetic method for coal mine detection. J Appl Geophys. 2019;169:165-173.
3. Wu X, Zhen QH, Chen WY, Teng F, Xue JJ, Wang YB. New Technologies for transient electromagnetic measurement with high performance. J Appl Geophys. 2025;233:105627.
4. Zhao HT, Liu LH, Wu K, Qi YZ, Fang GY. Constant Voltage-clamping Bipolar Pulse Current Source for Transient Electromagnetic System. Electr Power Compon Syst. 2013;41:960-971.
5. Jang C, Sin O, Jon G. Quantitative suppression of unsteady powerline noise in transient electromagnetic surveys: Adjustment of base-frequency and optimal choice of stacking-times. Rev Sci Instrum. 2024;95:104504.
6. Yu CG, Fu ZH, Zhang HQ, Tai HM, Zhu XG. Transient process and optimal design of receiver coil for small-loop transient electromagnetics. Geophys Prospect. 2014;62:377-384.
7. Xue GQ, Yan YJ, Li X, Di QY. Transient electromagnetic S-inversion in tunnel detection. Geophys Res Lett. 2007;34:L18403.